

# Measurement of the magnetic induction vector in superconductors using a double-layer Hall sensor array

Y. Abulafia, M. McElfresh,<sup>a)</sup> A. Shaulov, and Y. Yeshurun

Department of Physics, Institute for Superconductivity, Bar-Ilan University, Ramat-Gan, Israel

Y. Paltiel, D. Majer, H. Shtrikman, and E. Zeldov

Department of Condensed Matter Physics, Weizmann Institute, 76100 Rehovot, Israel

(Received 19 December 1997; accepted for publication 2 April 1998)

We describe an experimental technique for simultaneous measurement of both the normal ( $B_z$ ) and the in-plane ( $B_x$ ) components of the magnetic induction field near the surface of a superconducting sample. This technique utilizes a novel design of a double-layered Hall sensor array fabricated from a GaAs/AlGaAs heterostructure containing two parallel layers of a two-dimensional electron gas. The effectiveness of this technique is demonstrated in measurements of  $B_x$  and  $B_z$  and the current distribution at the surface of a thin YBa<sub>2</sub>Cu<sub>3</sub>O<sub>7</sub> crystal. © 1998 American Institute of Physics. [S0003-6951(98)04322-8]

In recent years small Hall sensors and linear arrays of hall sensors have been instrumental in studying the magnetic properties of superconducting materials.<sup>1-6</sup> Specifically, Hall sensor arrays have been effectively utilized in the study of magnetic phase diagram<sup>2-4</sup> and flux dynamics<sup>5,6</sup> in high temperature superconductors (HTS). A typical experimental configuration is described in Fig. 1. The sample is typically a long, flat uniform strip of material with the linear sensor array running perpendicular to the length of the strip. The Hall sensors measure the component  $B_z$  of the induction field normal to the surface, as a function of the position  $x$ . It has been shown<sup>1-6</sup> that the induction profiles  $B_z(x)$ , and their time evolution, contain ample information on the static and dynamics of the vortex state in HTS. However, in many cases it is important to measure not only the normal component  $B_z$  but also the in-plane component  $B_x$ . For example, it has been shown<sup>7</sup> that accurate interpretation of magnetic relaxation data in thin platelet samples requires the knowledge of both  $B_z$  and  $B_x$ , as both of these components exhibit relaxation, and the relaxation of each component is coupled to that of the other. The in-plane component  $B_x$  also plays an important role in determination of the current distribution  $J_y(x)$  within the sample. The current density is related to the gradients of  $B_x$  and  $B_z$  through the Maxwell equation:

$$J_y(x,z) = -\frac{c}{4\pi} \left( \frac{\partial B_z}{\partial x} - \frac{\partial B_x}{\partial z} \right). \quad (1)$$

For thin samples, which are frequently the shape of anisotropic high-temperature superconductors, the contribution of the  $B_x$  term dominates as usually  $\partial B_x / \partial z \gg \partial B_z / \partial x$ .<sup>8,9</sup>

The in-plane component  $B_x$  can be indirectly calculated from the  $B_z$  data using a two-step procedure: First, an inversion scheme<sup>10,11</sup> is employed to calculate the current distribution  $J_y(x)$  from the  $B_z(x)$  data. In the second step,  $B_x$  can be calculated from  $J_y(x)$ , using the Biot-Savart formula,

$$\mathbf{B}(\mathbf{r}) = \frac{1}{c} \int \frac{\mathbf{J}(\mathbf{r}') \times (\mathbf{r} - \mathbf{r}')}{|\mathbf{r} - \mathbf{r}'|^3} d^3\mathbf{r}', \quad (2)$$

where  $\mathbf{r}$  indicates the location where  $B$  is measured. In this procedure the accuracy of the calculated  $B_x$  values is affected by the limited number of  $B_z$  data points and by the accuracy of the measured  $B_z$  values.

In this letter we describe a direct experimental method for measuring  $B_x$  and  $B_z$  simultaneously. As we show below, measurements of these two components in thin films allow a direct determination of the current distribution.

Experimental methods for measurements of both  $B_x$  and  $B_z$  were previously described by Kvitkovich and Majoros<sup>12</sup> and by Vlasko-Vlasov *et al.*<sup>13</sup> The device of Kvitkovich and Majoros comprises three independent Hall sensors arranged in such a manner that their active areas are placed in three mutually perpendicular planes. This method requires significant separation between the sample surface and the sensors. In addition, measurement of the field distribution requires mechanical scanning of the device. The method of Vlasko-Vlasov *et al.* utilizes domain wall motion in the magneto-optic indicator. Application of this method is complicated by the fact that it requires an application of an external in-plane field with variable intensity to match the local values of  $B_x$ .

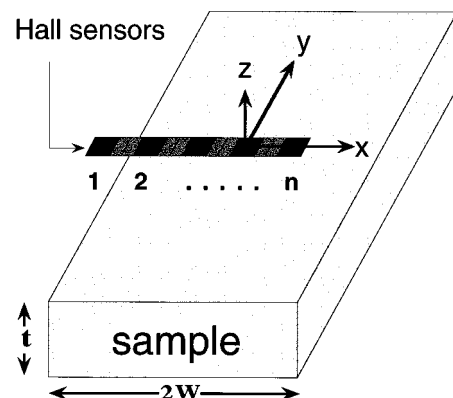


FIG. 1. Schematic configuration of the Hall sensor array relative to the sample.

<sup>a)</sup>Permanent address: Department of Physics, Purdue University, West Lafayette, IN 47907. Work was done while on a sabbatical at The Weizmann Institute and Bar Ilan University.

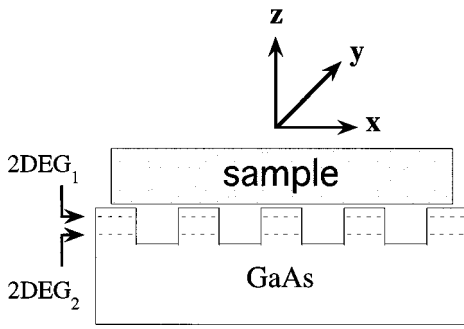


FIG. 2. Schematic diagram of a two-layer Hall sensor array fabricated from an AlGaAs/GaAs heterostructure containing two parallel two-dimensional electron gas layers separated by approximately  $1 \mu\text{m}$  of AlGaAs and GaAs.

In this work we propose an advanced approach, based on double-layer hall arrays, which allows measurement of *both*  $B_z$  and  $B_x$  close to the sample surface. It has the advantages provided by a stationary sensor array, i.e., it can be in direct contact with the sample and can be scanned electronically, and in addition, it does not require the application of an external in-plane field.

The specific implementation of our method, see Fig. 2, is based on fabrication of GaAs/AlGaAs heterostructure containing two distinct two-dimensional electron gas (2DEG) layers. The separation between the layers is  $\sim 1 \mu\text{m}$ . It is noteworthy that the number of Hall sensor layers can be increased at will. The present work demonstrates the basic principle by a two-layer device. Using this configuration it is possible to measure the distribution of  $B_z(x)$  at two different distances  $z$  from the sample surface, thereby allowing the gradient  $\partial B_z / \partial z$  to be determined at a series of  $x$  values. For the common experimental configuration described in Fig. 1, in which the sample is long in the  $y$  direction, the Gauss law  $\nabla \cdot \mathbf{B} = \partial B_x / \partial x + \partial B_z / \partial z = 0$ , leads to

$$\int_0^x \frac{\partial B_z(x')}{\partial z} dx' = -B_x(x) + B_x(0), \quad (3)$$

where  $x=0$  is the center of the sample and  $B_x(x)$  is the value of the in-plane component close to the sample surface. For antisymmetric current density distribution, i.e.,  $J_y(x) = -J_y(-x)$ , present in magnetization measurements, the integration constant  $B_x(0)=0$ .

In thin films, the knowledge of  $B_x$  directly yields the current distribution across the sample. In this case  $\partial B_x / \partial z \gg \partial B_z / \partial x$ , and thus the integration of Eq. (1) over the sample thickness yields the sheet current

$$I_y(x) = (c/2\pi)B_x(x), \quad (4)$$

where  $B_x(x)$  is the field at the surface of the sample induced by the current sheet.

The heterostructure was grown in a Riber model 32 molecular beam epitaxy system, under conventional growth conditions, on an undoped semi-insulating (100) oriented GaAs substrate. The buffer layer consists of an AlGaAs/GaAs superlattice as well as thick undoped GaAs. A 30 nm spacer of AlGaAs separates each of the 2DEG from the Si-doped ( $2 \times 10^{18} \text{ cm}^{-3}$ ) AlGaAs layer which supplies the 2DEG with carriers. The 2DEGs are separated from each other by a  $1 \mu\text{m}$  thick layer of AlGaAs and GaAs designed

to allow formation of two isolated Ohmic contacts, and to avoid the existence of a parasitic 2DEG between the two gases. The top 2DEG lies about 100 nm beneath the sample surface. The structure is capped by 10 nm of undoped AlGaAs and a 15 nm of undoped GaAs to reduce the leakage from the surface. A schematic illustration of the double 2DEG structure is given in Fig. 2.

The fabrication process<sup>14</sup> of the double-layer Hall sensor consists of the following steps using standard clean room processes. A first mesa is defined which creates holes through the upper 2DEG to allow evaporation of Ohmic contacts to the lower 2DEG. Using a lift-off process, an Ohmic contact to the lower 2DEG is evaporated (Ni/GeAu/Ni/Au) and alloyed at 450 °C. A second lift-off process and evaporation of Ni/GeAu/Nb/Au for Ohmic contacts to the upper 2DEG is then carried out and alloyed at 390 °C. The Nb layer and the lower alloying temperature prevent the upper Ohmic contact from making shorts to the lower 2DEG. Finally, a mesa defining the Hall sensors in both layers is etched either chemically or by reactive ion etching.

For the present study, a linear Hall sensor array containing five pairs of elements was fabricated, each element having an active area of  $10 \mu\text{m} \times 10 \mu\text{m}$ , separated by  $40 \mu\text{m}$  between centers. The upper and lower 2DEGs had carrier densities of  $5 \times 10^{11}$  and  $3.5 \times 10^{11} \text{ cm}^{-2}$ , respectively, as measured at 80 K by the Hall voltage. The corresponding carrier mobilities of 96 000 and 137 000  $\text{cm}^2/\text{V s}$  were obtained from resistivity measurements at 80 K and zero magnetic field. The upper and lower 2DEG layers had sensitivities of about 0.14  $\Omega/\text{G}$  and 0.20  $\Omega/\text{G}$ , respectively. The noise level was approximately 0.5 G. For the magnetic measurements 100  $\mu\text{A}$  driving current was applied to each layer using two separate current sources, with the current in each source switched in polarity in order to eliminate offset potentials.

The sample measured was a detwinned thin  $\text{YBa}_2\text{Cu}_3\text{O}_7$  single crystal with dimensions of  $1500 \times 480 \times 15 \mu\text{m}^3$ . The sample was measured at  $T = 50 \text{ K}$  where the magnetotransport behavior can be characterized by the Bean critical state model. The sample was repositioned several times on the sensor array in order to produce a complete  $B_z(x)$  profile across the complete width of the sample. The experimental procedure involved cooling the sample in zero field, then stabilizing the temperature, after which a magnetic field  $H > 2H^*$  was applied, where  $H^*$  is the field of complete flux penetration. The field was reduced to zero prior to the collection of the data.

Shown in Fig. 3 (circles) is a typical field profile  $B_z(x)$  measured in the remanent state ( $H=0$ ). Also shown in Fig. 3 (squares) is the profile of the planar component  $B_x(x)$  as calculated using Eq. (3) with  $B_x(0)=0$ , assuming antisymmetric current distribution. According to Eq. (4) the sheet current  $I_y(x)$  is proportional to  $B_x$ . Thus, the  $B_x$  profile shown in Fig. 3 also represents the current profile  $I_y(x)$  as indicated by the right-hand side ordinate. Note that  $I_y(x)$  in the remanent state is not constant, a fact that is usually ignored in calculations. This determination of  $I_y(x)$  can now be used to calculate  $B_x(x)$  and  $B_z(x)$  using Eq. (2) as a self-consistency check. The calculated values are shown in Fig. 3 as solid and dashed lines, respectively. It can be seen

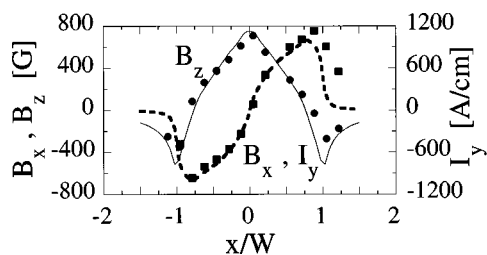


FIG. 3. Measured profiles  $B_z(x)$  and  $B_x(x)$  near the surface of a YBCO thin crystal using a double-layer Hall sensor array. Solid and broken lines are calculated profiles. The squares describe both  $B_x(x)$  (left ordinate) and  $I_y(x)$  (right ordinate) which are related through Eq. (4).

that the calculated profiles are in good agreement with the measured ones. This supports the validity of our method and measurements.

In conclusion, we described a novel method for a simultaneous measurement of both the in-plane and the normal component of the induction field near the surface of a sample. A knowledge of these two components allows determination of the current distribution across the sample. We have demonstrated this technique for measurements of  $B_x$ ,  $B_z$ , and the current distribution in a thin superconducting  $\text{YBa}_2\text{Cu}_3\text{O}_7$  crystal in a remanent state. However, our method is more general and may be applicable in characterization of other sources of magnetic fields and currents. Application of this method for detection of defects in a sample, by mapping the distribution of electric currents, will be published elsewhere.

This work was supported in part by the USA-Israel Binational Science Foundation, by the Heinrich Hertz Minerva Center, and by the Israel Science Foundation. One of the authors (M.M.) was supported by the Director for Energy Research, Office of Basic Energy Sciences through the Midwest Superconductivity Consortium (MISCON) DOE Grant No. DE-FG02-90ER45427 and in part by the Materials Research Science and Engineering Center (MRSEC) Program of the National Science Foundation under Award No. DMR-9400415.

- <sup>1</sup>H. W. Weber, G. P. Westphal, and I. Adaktylos, *Cryogenics* **16**, 39 (1976); T. Tamegai, L. Krusin-Elbaum, P. Santhanam, M. J. Brady, W. T. Masselink, C. Feild, and F. Holtzberg, *Phys. Rev. B* **45**, 2589 (1992); M. Konczykowski, L. Burlachkov, Y. Yeshurun, and F. Holtzberg, *Physica C* **194**, 155 (1992); A. M. Chang, H. D. Hallen, L. Harriot, H. F. Hess, H. L. Kao, J. Kwo, R. E. Miller, R. Wolfe, J. van der Ziel, and T. Y. Chang, *Appl. Phys. Lett.* **61**, 1974 (1992); T. Tamegai, Y. Iye, I. Oguro, and K. Kishio, *Physica C* **213**, 33 (1993); D. A. Brawner and N. P. Ong, *J. Appl. Phys.* **73**, 3890 (1993); S. T. Stoddart, S. J. Bending, A. K. Geim, and M. Henini, *Phys. Rev. Lett.* **71**, 3854 (1993); A. Oral, S. J. Bending, and M. Henini, *Appl. Phys. Lett.* **61**, 1974 (1996).
- <sup>2</sup>E. Zeldov, A. I. Larkin, V. B. Geshkenbein, M. Konczykowski, D. Majer, B. Khaykovich, V. M. Vinokur, and H. Shtrikman, *Phys. Rev. Lett.* **73**, 1428 (1994); E. Zeldov, D. Majer, M. Konczykowski, V. B. Geshkenbein, V. M. Vinokur, and H. Shtrikman, *Nature (London)* **375**, 373 (1995).
- <sup>3</sup>B. Khaykovich, E. Zeldov, D. Majer, T. W. Li, P. H. Kes, and M. Konczykowski, *Phys. Rev. Lett.* **76**, 2555 (1996); B. Khaykovich, M. Konczykowski, E. Zeldov, R. Doyle, D. Majer, P. H. Kes, T. W. Li, *Phys. Rev. B* **56**, R517 (1997).
- <sup>4</sup>D. Giller, A. Shaulov, R. Prozorov, Y. Abulafia, Y. Wolfus, L. Burlachkov, Y. Yeshurun, E. Zeldov, V. M. Vinokur, J. L. Peng, and R. L. Greene, *Phys. Rev. Lett.* **79**, 2542 (1997).
- <sup>5</sup>Y. Abulafia, A. Shaulov, Y. Wolfus, R. Prozorov, L. Burlachkov, Y. Yeshurun, D. Majer, E. Zeldov, and V. M. Vinokur, *Phys. Rev. Lett.* **75**, 2404 (1995); Y. Abulafia, A. Shaulov, Y. Wolfus, R. Prozorov, L. Burlachkov, Y. Yeshurun, D. Majer, E. Zeldov, H. Wuhl, V. B. Geshkenbein, and V. M. Vinokur, *Phys. Rev. Lett.* **77**, 1596 (1996).
- <sup>6</sup>Y. Abulafia, D. Giller, Y. Wolfus, A. Shaulov, Y. Yeshurun, D. Majer, E. Zeldov, J. L. Peng, and R. L. Greene, *J. Appl. Phys.* **81**, 4944 (1997).
- <sup>7</sup>Y. Abulafia, A. Shaulov, Y. Wolfus, R. Prozorov, L. Burlachkov, D. Majer, E. Zeldov, V. M. Vinokur, and Y. Yeshurun, *J. Low Temp. Phys.* **107**, 455 (1997).
- <sup>8</sup>E. H. Brandt and M. Indenbom, *Phys. Rev. B* **48**, 12 893 (1993).
- <sup>9</sup>E. Zeldov, J. R. Clem, M. McElfresh, and M. Darwin, *Phys. Rev. B* **49**, 9802 (1994).
- <sup>10</sup>E. H. Brandt, *Phys. Rev. B* **46**, 8628 (1992).
- <sup>11</sup>R. J. Wijngaarden, H. J. W. Spoelder, R. Surdeanu, and R. Griessen, *Phys. Rev. B* **54**, 6742 (1996).
- <sup>12</sup>J. Kvitkovich and M. Majoros, *J. Magn. Magn. Mater.* **157/158**, 440 (1996).
- <sup>13</sup>V. K. Vlasko-Vlasov, L. A. Dorosinskii, M. V. Indenbom, V. I. Nikitenko, A. A. Polyanskii, and R. L. Prozorov, *Supercond., Phys. Chem. Technol.* **6**, 555 (1993).
- <sup>14</sup>Y. Abulafia, Y. Wolfus, A. Shaulov, Y. Yeshurun, E. Zeldov, D. Majer, and H. Shtrikman (patent pending).